

# Structural change of keratin protein in human hair by permanent waving treatment†

Naoki Nishikawa<sup>a,b,\*</sup>, Yoshiaki Tanizawa<sup>a</sup>, Shoichi Tanaka<sup>a</sup>,  
 Yasunobu Horiguchi<sup>a</sup> and Tetsuo Asakura<sup>b</sup>

<sup>a</sup>Analytical Research Center, Lion Corp., 13-12, Hirai 7-chome, Edogawa-ku, Tokyo 132, Japan

<sup>b</sup>Department of Biotechnology, Tokyo University of Agriculture and Technology, Nakacho 2-chome, Koganei, Tokyo 184, Japan

(Received 15 October 1997; revised 6 November 1997; accepted 13 November 1997)

The damage to human hair caused by permanent waving treatment was examined from the viewpoint of structure with several spectroscopic methods, <sup>13</sup>C CP/MAS n.m.r., wide angle X-ray diffraction (WAXD), FTi.r. and Raman methods. The partial disruption of  $\alpha$ -helical structure constituting the microfibril in hair fibre was revealed by this study, although the incomplete re-oxidation of the disulphide bond has been considered to be the main damage caused by the treatment. Moreover, this disruption was mainly caused in the first reduction process. In particular, <sup>13</sup>C CP/MAS n.m.r. gave the quantitative evaluation for change of  $\alpha$ -helical content in the microfibril with permanent waving treatment. In addition, FTi.r. and Raman spectra indicated that the  $\alpha$ -helix was partially changed to random coil, rather than to  $\beta$ -sheet structure. © 1998 Elsevier Science Ltd. All rights reserved.

(Keywords: keratin protein;  $\alpha$ -helix structure in microfibril; permanent waving treatment)

## INTRODUCTION

Like wool, nail and horn, human hair is one of the mammalian structural components formed from  $\alpha$ -keratin<sup>1,2</sup>. The histological structure of hair fibre consists of two components, cortex and cuticle. The cortex comprising 85–90% of hair<sup>3,4</sup> seems to be responsible for most physical and mechanical properties of hair. This component consists of spindle-shaped macrofibrils which have two main structures, microfibril and matrix, which are distinguished by their structures and amino acid compositions<sup>1–7</sup>. The microfibril is a crystalline fibrous protein which is mainly composed of  $\alpha$ -helical proteins with low content of cystine. These structures are aligned along the fibre axis and embedded in an amorphous matrix with a high cystine content constituting disulphide cross-linkage. Thus, hair fibre is regarded as an oriented fibre in which the crystalline filaments are aligned.

It is generally known that the physical and mechanical properties of hair fibre are changed by chemical cosmetic treatments such as permanent waving, bleaching or dyeing<sup>3,8–13</sup>. In every treatment, the damage to these properties has been regarded as the result of disruption of the disulphide bond in the constituent protein of hair. For example, permanent waving treatment consists of two different processes, the reducing process and the oxidizing process<sup>14,15</sup>. The first process is intended to act chemically on the covalent disulphide bond. The hair is wetted with thiol aqueous solution and rolled on curlers so that the imposed deformation of hair is in the shape of curls. In

the second process, the curls are set by restoring the initial chemical structure to the fibre. The thiol group of keratin protein which is produced in the first process is re-oxidized into the disulphide bond. It is generally known that an incomplete re-oxidation of the disulphide bond in keratin protein occurs in the second process<sup>16–21</sup>. This incomplete re-oxidation has been considered to be the main cause of the physical and mechanical properties of the hair fibre being not as good as those of untreated hair. However, the permanent waving treatment is also expected to cause change in the ordered structure of the microfibril oriented along the fibre axis. Therefore, it is necessary to clarify the structure and structural change of the microfibril in human hair before and after permanent waving treatment<sup>22</sup>.

In this study, the structure of the keratin protein constituting human hair and the structural change caused by permanent waving treatment (reduction followed by oxidation) were studied using <sup>13</sup>C CP/MAS n.m.r., wide-angle X-ray diffraction (WAXD), and Raman and infrared (i.r.) techniques in order to examine carefully any damage other than the incomplete re-oxidation of the disulphide bond, reported previously.

Thus far, X-ray diffraction and i.r. methods have been used to study the fibre structure<sup>3,23–26</sup>. Recently, solid state n.m.r. has been successfully applied to the structural analysis of protein fibres such as silk fibroin<sup>27–31</sup> and wool keratin<sup>32–36</sup>. In particular, the <sup>13</sup>C and <sup>15</sup>N n.m.r. chemical shifts of these fibres are conformation-dependent, and therefore, the local structure such as the  $\alpha$ -helix and  $\beta$ -sheet in the fibre sample can be characterized with such chemical shift data. The fraction of the different local structure in the sample is easily evaluated from the relative peak intensities. Therefore, in this work, the quantitative interpretation of the structural change of keratin protein

\* To whom correspondence should be addressed

† This work was presented at the 44th Annual Meeting of the Society of Polymer Science, Japan; 1996, Nagoya, Japan.

with the treatment was performed using the  $^{13}\text{C}$  CP/MAS n.m.r. technique.

## EXPERIMENTAL

### Materials

Commercial black Asian hair from Staffs Co., Ltd., (Tokyo) was used for all experiments. Hair bundles were washed with a 1% solution of sodium dodecyl sulphate (SDS), rinsed thoroughly with deionized water and air-dried at room temperature. In the Raman experiment, natural white Asian hair was used in order to decrease the fluorescence.

The carboxymethyl derivative of keratin protein (SCMK) was extracted from the human hair, and then separated to a low sulphur fraction (SCMKA) and a high sulphur fraction (SCMKB), which corresponded to microfibril and matrix, respectively<sup>37,38</sup>. The air-dried hair was chopped and cleaned by extraction with hexane, ethanol and acetone three times in order to remove lipids from the hair. Then the chopped hair was wetted with 8 M urea, and reduced by 0.23 M 2-mercaptoethanol overnight at room temperature under nitrogen gas. Carboxymethylation of thiol groups in the hair keratin was performed by a treatment with 0.23 M iodoacetic acid for 15 min. The extract containing SCMK was filtered and dialysed for at least 24 h by changing deionized water several times. After the SCMK solution was adjusted to pH 4.4 with acetic acid, SCMKA was sedimented by centrifugation. This precipitate was dissolved in 50 mM sodium tetraborate solution. The SCMKA obtained was purified by re-precipitating twice at pH 4.4. The supernatant fraction containing the SCMKB was dialysed against deionized water and adjusted to pH 4.4 with 2 M acetate buffer. After centrifugation, the SCMKB was purified twice by the same process, and then these two fractions, SCMKA and SCMKB, were lyophilized.

Permanent waving, reduction followed by oxidation, of human hair was performed using the standard method<sup>13–15</sup>. The details of the treatment procedure and condition are described as follows. Hair bundles, wetted with deionized water, were soaked in a large excess of 7.0% (wt/wt) ammonium thioglycolic acid aqueous solution of pH 9.6 for 20, 30, 60, and 180 min at 35°C. Thus, the treatment time was changed. After being rinsed for 20 min under running deionized water, the hair bundles were neutralized in 2.1% (wt/wt) sodium bromate at pH 7.0 (oxidation process) for the same time as previous reducing process. Once again the hair bundles were rinsed under running water, followed by air-drying at room temperature.

### $^{13}\text{C}$ CP/MAS n.m.r. measurements

$^{13}\text{C}$  CP/MAS n.m.r. spectra were obtained with a GSX-400 n.m.r. spectrometer (JEOL Co., Tokyo) operating at a  $^{13}\text{C}$  frequency of 100.1 MHz equipped with a CP/MAS accessory. Hair (110 mg) was turned to powder, and poured into a cylindrical rotor made of zirconia. The spinning rate, contact time and repetition time were 6 KHz, 2 ms and 5 s, respectively. A spectral width of 27 KHz and a sampling point of 2 K were used for the spectral acquisition. Spectra were accumulated 6K times to achieve a reasonable signal-to-noise ratio. The  $^{13}\text{C}$  chemical shifts were referenced to the adamantane peak at 29.5 ppm relative to tetramethylsilane (TMS). Spinning side bands were removed by the TOSS (total suppression of sidebands) method.

### Wide-angle X-ray diffraction (WAXD) measurements

X-ray diffraction studies were made on an X-ray diffractometer (RIGAKU Co., Tokyo) equipped with a texture goniometer assembly. Approximately 20 hairs were fixed straight with texture clamps. Nickel-filtered  $\text{CuK } \alpha$  radiation ( $\lambda = 0.15406$  nm) generated at 40 kV and 40 mA was used. The incident beam was collimated through a collimator 100  $\mu\text{m } \phi$  and the diffraction beam was received through a 1.8 mm wide and 5.8 mm long slit. Diffraction patterns were obtained by continuous scan at a scan speed of  $0.02^\circ$  ( $2\theta$ ) per second. Most WAXD measurements were either equatorial, lying in a plane perpendicular to the hair axis, or meridional, lying in a plane parallel to the hair axis.

### FTi.r. measurements

FTi.r. measurements were performed with a JIR-6000 FT-IR spectrometer (JEOL Co., Tokyo). Hair samples were ground in liquid nitrogen<sup>39</sup>. The small amounts of ground hair samples were mixed with KBr crystal and pressed into pellets. The FTi.r. spectra were obtained after 500 scans at a resolution of  $4\text{ cm}^{-1}$  using Happ-Genzel apodization.

### Raman measurements

An NIR-1000 spectrometer (JASCO, Tokyo) was used for Raman measurements using 514.5 nm light from an Ar ion laser (NEC, Tokyo) and the data were collected at a power level, 100 mW. A piece of hair was mounted in the fibre cramp. The typical conditions for the Raman spectroscopy were as follows: entrance slit, 700  $\mu\text{m}$ ; intermediate slit, 750  $\mu\text{m}$ ; exit slit, 700  $\mu\text{m}$ ; slit height, 4 mm; scan speed, 2 s per div.; and repeat, 16 times<sup>40</sup>.

## RESULTS AND DISCUSSION

### Decrease of $\alpha$ -helix content by reduction/oxidation treatment monitored with WAXD

The change in the meridional WAXD pattern of human hair with reduction followed by oxidation treatment is shown as a function of the treatment time in *Figure 1*. The WAXD pattern of keratin fibre has been assigned by Pauling and Corey<sup>41</sup>. The diffraction peak at  $2\theta = 18^\circ$  (0.51 nm) was assigned to the repeat distance for the  $\alpha$ -helical chain corresponding to 3.6 amino acid residues. In addition, the tailing from  $2\theta = 20$ – $30^\circ$  was assigned to an amorphous halo inherent in general organic materials. Thus, the

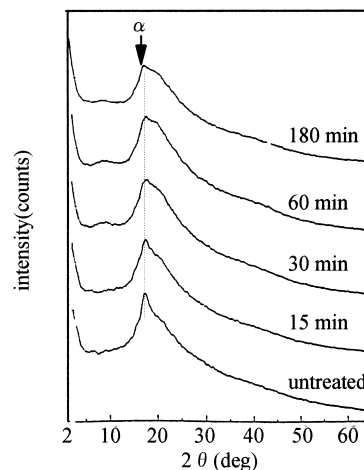


**Figure 1** Time dependence of the meridional WAXD pattern of human hair after permanent waving treatment. The time taken for reduction followed by oxidation treatment was changed

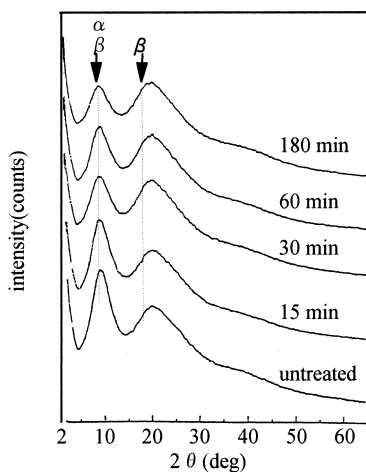


**Figure 2** Time dependence of the equatorial WAXD pattern of human hair after permanent waving treatment. The time taken for reduction followed by oxidation treatment was changed

presence of both  $\alpha$ -helix and amorphous domains is detected in the untreated human hair sample. The peak intensity at  $18^\circ$  decreases within the treatment time of 30 min and tends to be constant in the case of more than 30 min. Thus, the change of  $\alpha$ -helical structure occurs partly within a relatively short treatment time.

However, the change of equatorial WAXD pattern with reduction followed by oxidation is shown as a function of treatment time in *Figure 2*. The peak at  $2\theta = 19^\circ$  (0.47 nm) associated with  $\beta$ -sheet structure, and the peak at  $2\theta = 9^\circ$  (0.98 nm) was commonly assigned to both  $\alpha$ -helix and  $\beta$ -sheet structure<sup>42</sup>. The broad base-line from  $2\theta = 20\text{--}30^\circ$  was assigned to an amorphous halo detected inherently in organic materials which is similar to the meridional WAXD pattern (*Figure 1*). The peak intensity at  $2\theta = 9^\circ$  decreases with an increase of the treatment time, and the degree of decrease is remarkable until 30 min. This observation is the same as those of the meridional WAXD patterns, mentioned above. However, it is difficult to determine the change in the  $\alpha$ -helix content quantitatively from either the meridional or the equatorial diffraction pattern because the WAXD pattern depends on the orientation of the fibre.

#### Determination of $\alpha$ -helix content with reduction/oxidation treatment by $^{13}\text{C}$ CP/MAS n.m.r.

*Figure 3* shows  $^{13}\text{C}$  CP/MAS n.m.r. spectra of keratin samples: untreated hair, hair after 60 min permanent waving treatment and the SCMKA fraction. The details of peak assignments are given elsewhere<sup>33–35</sup>. The peak of the carbonyl, aromatic, C  $\alpha$  methine and side-chain aliphatic carbons appear at about 170–180, 115–160, 45–60 and 10–40 ppm, respectively. The high field region of 10–60 ppm is relatively complex because of the appearance of many peaks owing to the individual amino acid residues in keratin protein, although the change of the spectra can be observed between untreated and 60 min treated samples. However, the difference of peak shape in the carbonyl region was clearly observed. Therefore, the change in the keratin protein structure with reduction followed by oxidation treatment is monitored from the carbonyl carbon region. In order to confirm the assignment of the carbonyl carbon peak, the spectra of SCMKA and SCMKB corresponding to the microfibril and matrix separated from hair, respectively, are shown in *Figure 4*. Since the former mainly takes  $\alpha$ -helix structure and the latter, random-coil structure, which

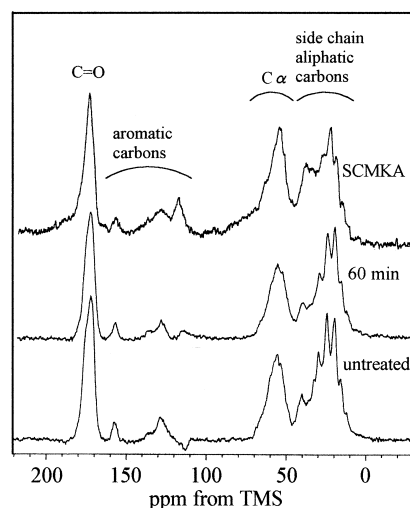


**Figure 3**  $^{13}\text{C}$  CP/MAS n.m.r. spectra of untreated hair and hair treated by permanent waving for 60 min, and the SCMKA fraction from human hair. The details of the peak assignments are given elsewhere<sup>33–35</sup>

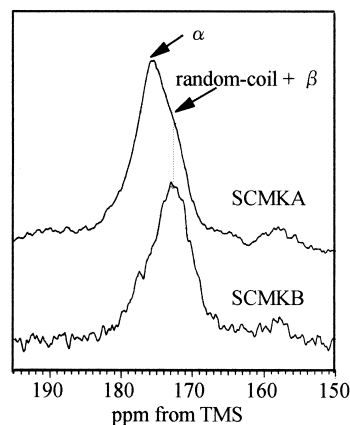


**Figure 4**  $^{13}\text{C}$  CP/MAS n.m.r. spectra for the carbonyl carbon region of the SCMKA and SCMKB fractions from human hair

has been confirmed with TG and X-ray analyses<sup>26</sup>, the peak at 176 ppm in the SCMKA spectrum can be assigned to the  $\alpha$ -helix and the peak at 172 ppm in the SCMKB spectrum to the random-coil. The carbonyl carbon chemical shift of the  $\alpha$ -helix in human hair is the same as that in wool keratin<sup>33</sup>. Generally, the chemical shifts of the  $\alpha$ -helix structure should depend on the individual amino acid residues in the protein, but the range of such a chemical shift dispersion is considered to be within the line width in this work. Namely, the chemical shifts depend strongly upon the secondary structure. The high field shoulder observed in the SCMKA spectrum at around 172 ppm (*Figure 4*) is assigned to the random coil structure in the sample. However, the chemical shift of the  $\beta$ -sheet structure is also assigned to the random coil structure. In addition, the peak at 172 ppm is also observed in the  $^{13}\text{C}$  CP/MAS n.m.r. spectrum of human hair where the  $\beta$ -sheet structure is clearly present, as shown in the equatorial WAXD pattern (*Figure 2*). Therefore, the peak at 172 ppm should be assigned to both the  $\beta$ -sheet and random coil structures. As mentioned below, the structural change with reduction followed by oxidation treatment is considered to be an  $\alpha$ -helix  $\rightarrow$  random-coil structure rather than an  $\alpha$ -helix  $\rightarrow$  sheet-structure from IR and Raman studies.

*Figure 5* shows the carbonyl carbon spectra of human hair

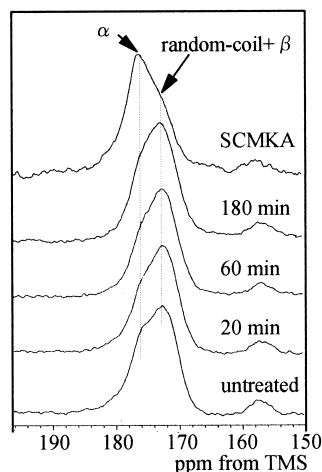


**Figure 5** Time dependence of the carbonyl carbon region in  $^{13}\text{C}$  CP/MAS n.m.r. spectra of human hair after permanent waving treatment. The time taken for reduction followed by oxidation treatment was changed. The details are given in the text

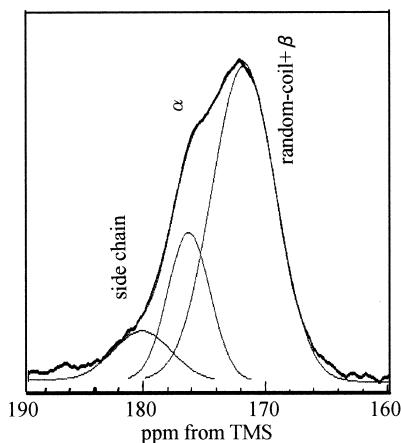


**Figure 6**  $^{13}\text{C}$  CP/MAS n.m.r. spectrum of the carbonyl carbon region of human hair. The spectral simulation was performed, assuming a Gaussian line shape. The simulated results are summarized in Table 1

with the reduction followed by oxidation treatment as a function of treatment time along with the peak of SCMKA. The relative intensity of the peak at 176 ppm assigned to the  $\alpha$ -helix decreased by 20 min treatment, but no significant decrease was observed after further treatment. In order to determine quantitatively the  $\alpha$ -helix content during treatment, a spectral simulation assuming Gaussian line shape was performed. As an example, the observed and deconvoluted peaks of carbonyl carbon of the untreated hair are shown in Figure 6. Here, the small broad peak at around 180 ppm was assumed to be the carbonyl carbon of the side-chain of the amino acid residues such as Glu, Asp and carboxymethyl-L-cysteine<sup>33</sup>.

The change in the  $\alpha$ -helix content with reduction followed by oxidation is summarized in Table 1. The ratio of the peak area at 172 ppm versus total peak area was calculated as the  $\alpha$ -helix content in hair fibre. The  $\alpha$ -helix content of the untreated human hair is calculated as 23.7%, which is considerably smaller than the helix content, 42.0% for wool keratin<sup>33</sup>. This comes from the difference in the fraction of SCMKA between wool and hair keratins: 75% for wool<sup>33</sup> and 65% for human hair<sup>43</sup>. The  $\alpha$ -helix content decreased from 23.7 to 20.7% during the first 20 min treatment, and did not change during further treatment. This

**Table 1** The change in the fraction of  $\alpha$ -helix, and  $\beta$ -sheet and random-coil in human hair by permanent waving treatment (reduction followed by oxidation) determined from the carbonyl carbon peaks in the  $^{13}\text{C}$  CP/MAS n.m.r. spectra of human hair

Treatment	$\alpha$ -helix	$\beta$ -sheet and random-coil
Untreated	23.7	76.3
20 min	20.7	79.3
60 min	20.4	79.6
180 min	20.7	79.3

The spectral simulation was performed, assuming a Gaussian line shape

result supported the conclusion obtained by the WAXD studies (Figures 1 and 2).

#### Change in the $\alpha$ -helix content during individual reduction and oxidation steps monitored with $^{13}\text{C}$ CP/MAS n.m.r. and WAXD

The meridional WAXD patterns and the carbonyl carbon region in the  $^{13}\text{C}$  CP/MAS n.m.r. spectra during individual reduction and oxidation steps are shown in Figure 7A and B, respectively, in order to check the stage where the structural change occurs. The peak at  $2\theta = 18^\circ$  assigned to  $\alpha$ -helix in the meridional WAXD pattern decreased at the reduction process. Similarly the decrease of the shoulder at around 176 ppm in  $^{13}\text{C}$  CP/MAS n.m.r. spectra assigned to the carbonyl carbon of the  $\alpha$ -helix structure also occurs at the reduction process. No spectral change is observed at the oxidation step after the reduction step. These results indicate that the change of the  $\alpha$ -helix structure in the microfibril occurs predominantly in the reduction step.

#### Structural change of human hair with reduction/oxidation treatment monitored with FTi.r. and Raman methods

Although X-ray diffraction and  $^{13}\text{C}$  CP/MAS n.m.r. studies revealed that change in the  $\alpha$ -helix structure in microfibril occurs at the reduction step, it is still uncertain whether the change is due to the formation of the random-coil or the  $\beta$ -sheet structure. It is difficult to get such information using the  $^{13}\text{C}$  CP/MAS n.m.r. method because of the overlapping of the peaks owing to the  $\beta$ -sheet and random-coil structures at around 172 ppm (Figure 3). Similarly, the equatorial WAXD method presents difficulties because the peak  $2\theta = 19^\circ$  assigned to the  $\beta$ -form overlaps is concealed by the broad peak of the amorphous halo (Figure 2). Therefore, FTi.r. and Raman spectra are observed. The change in the i.r. spectrum of human hair caused by reduction followed by oxidation treatment along with the spectrum of SCMKA is shown in Figure 8. The absorptions at  $1530\text{ cm}^{-1}$ ,  $1537\text{ cm}^{-1}$  and  $1545\text{ cm}^{-1}$  in the Amide II region were assigned to the  $\beta$ -sheet, random-coil and  $\alpha$ -helix structure, respectively<sup>44</sup>. The i.r. spectrum of SCMKA is used as reference absorption for the  $\alpha$ -helix structure. A slight increase of the absorption at  $1537\text{ cm}^{-1}$ , owing to the random-coil, is observed after 60 min treatment time, in contrast with the slight decrease of the shoulder at  $1545\text{ cm}^{-1}$  owing to the  $\alpha$ -helix structure. The absorption region of  $\beta$ -sheet is scarcely changed by the treatment.

Raman spectra are also obtained for the same purpose. This method has often been used for structural analysis of proteins, and the C–C stretching vibration of the main chain around  $950\text{ cm}^{-1}$  is a useful region<sup>45,46</sup> for this work. In the Raman experiment, the fluorescence owing to the impurities in the samples is often emitted during measurement and

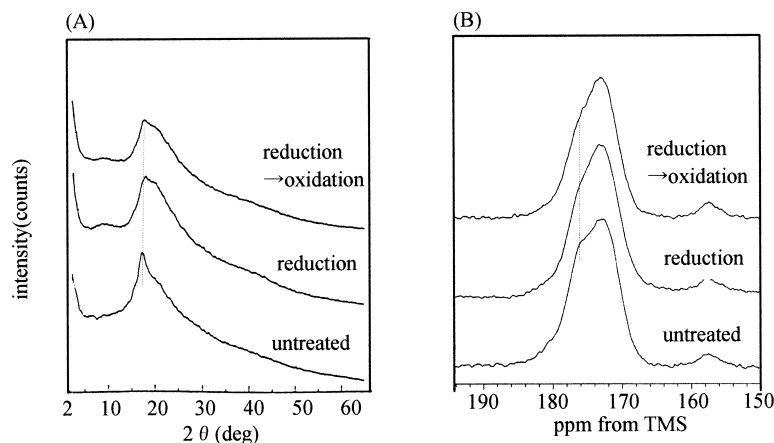


**Figure 7** The meridional WAXD patterns (A) and  $^{13}\text{C}$  CP/MAS n.m.r. spectra (the carbonyl carbon region) and (B) of human hair after individual reduction and oxidation process. The details are given in the text

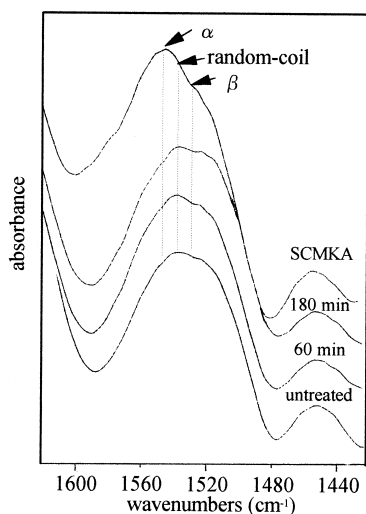


**Figure 8** Time dependence of the amide II region in the FTi.r. spectra of human hair after permanent waving treatment. The time taken for reduction followed by oxidation was changed. The spectrum of the SCMKA fraction is shown for reference as an  $\alpha$ -helix structure

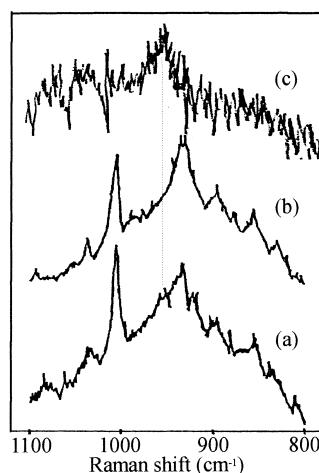


**Figure 9** Change in the C–C vibration of the main chain in Raman spectra of human hair before and after permanent-waving-treatment reduction followed by oxidation. (a) treated for 60 min, (b) untreated and (c) difference spectra (a) – (b)

obscures the normal spectra. Although the black hair emitted this fluorescence, Tanaka was able to obtain the normal spectrum under decreased fluorescence conditions using natural white hair<sup>40</sup>. In this study, therefore, the region of the C–C stretching vibration of main chain was analyzed with natural white hair. Raman spectra of the hair treated by reduction followed by oxidation treatment for 60 min and untreated hair are shown in *Figure 9*. The difference in the spectra between treated, *a*, and untreated, *b*, hair was small, but a shoulder was detected at around  $955\text{ cm}^{-1}$  in the spectrum of the treated hair, *a*. The difference between the treated- and untreated-hair spectra,  $c = a - b$ , was calculated referring to the peak intensity of the phenyl ring vibration at  $1010\text{ cm}^{-1}$  which was hardly affected by the structural change. In the C–C vibration region of the main chain, the peak corresponding to the  $\alpha$ -helix structure should be detected at  $900\text{--}945\text{ cm}^{-1}$  and the random-coil structure is detected at  $950\text{--}960\text{ cm}^{-1}$ . Usually, the peak of the  $\beta$ -sheet structure is scarcely detected because of its very weak intensity. The peak in the difference spectrum, *c*, was observed at around  $955\text{ cm}^{-1}$ , indicating Raman shift for a random-coil structure. Thus, the random-coil structure is increased by the reduction followed by oxidation treatment.

The result from FTi.r. and Raman spectrometry indicated that the  $\alpha$ -helix structure in the microfibril was changed to the random-coil structure by reduction followed by oxidation, rather than to the  $\beta$ -sheet structure.

## CONCLUSIONS

The fraction of  $\alpha$ -helix in the microfibril of human hair decreased slightly with permanent waving treatment (reduction followed by oxidation). The  $\alpha$ -helix was changed to the random-coil structure within a relative short treatment time. In general, it is known that changes in the physical properties such as decrease in the tensile strength are caused by permanent waving treatment. It has been recognized that such changes result from the incomplete re-oxidation of the disulphide bond existing mostly in the matrix of human hair. However, our study shows that, in addition to the incomplete re-oxidation of the disulphide bond, the decrease in  $\alpha$ -helix content in the microfibril might also be an origin of some of the damage. Solid state  $^{13}\text{C}$  n.m.r. can easily be used to monitor the structural change of human hair and therefore, solid state n.m.r. can be used to clarify the aspects of the damage of human hair with permanent waving.

ACKNOWLEDGEMENTS

We thank Dr. Hiroaki Yoshimizu of the Nagoya Institute of Technology and Prof. Isao Ando of the Tokyo Institute of Technology for helpful discussions. The expert technical support provided by Ms. Sachiko Tanaka and Mr. Ryo Kon have been invaluable. T.A. acknowledges support from Iwatani Science Foundation Japan and the Grant-in-Aid of the Ministry of Education, Science and Culture of Japan (grant no. 09450357).

REFERENCES

1. Gillespie, J. M., *Biochemistry and Physiology of the Skin*, Vol 1, ed. L. A. Goldsmith. Oxford University Press, New York, 1983, pp. 475–510.
2. Gillespie, J. M., *Cellular and Molecular Biology of Intermediate Filaments*, eds R. A. Goldman and P. M. Steinert. Plenum Press, New York, 1990, pp. 95–128.
3. Robbins, C. R., *Chemical and Physical Behavior of Human Hair*, 3rd edn. Springer-Verlag, New York, 1994.
4. Robbins, C. R. and Kelly, C. H., *Textile Res. J.*, 1970, **40**, 819.
5. Gillespie, J. M. and Marshall, R. C., *Hair Research*, eds C.E. Orfanos, Springer, Berlin, 1981, 76.
6. Menefee, E., *J. Soc. Cosmet. Chem.*, 1985, **36**, 17.
7. Arai, K., *Sen-i Gakkaishi*, 1989, **45**(12), 512.
8. Beyak, R., Mayer, C. F. and Kass, B. S., *J. Soc. Cosmet. Chem.*, 1969, **20**, 615.
9. Horiuchi, T., Ichinose, N. and Kashiwa, I., *J. Soc. Cosmet. Chem. Jpn.*, 1980, **14**(2), 116.
10. David, W. C., *J. Soc. Cosmet. Chem.*, 1978, **29**, 685.
11. Horiuchi, T., *Fragrance J.*, 1990, **12**, 69.
12. Worthmann, F. J. and Zahn, H., *Textile Res. J.*, 1994, **64**(12), 737.
13. Busch, P., Thiele, K., Fischer, D. and Hollenberg, D., *Cosmetics and Toiletries*, 1996, **111**, 41.
14. Zviak, C., 'Permanent Waving and Hair Straightening', *The Science of Hair Care*. Marcel Dekker Inc., New York, 1986, p. 183.
15. Inoue, K., *J. Soc. Cosmet. Chem. Jpn.*, 1994, **28**(3), 223.
16. Zahn, H., Gerthsen, T. and Kehren, K. L., *J. Soc. Cosmet. Chem.*, 1963, **14**(11), 531.
17. Robbins, C. R., *J. Soc. Cosmet. Chem.*, 1969, **20**, 555.
18. Gumprecht, J. G. and Patel, K., *J. Soc. Cosmet. Chem.*, 1977, **28**, 717.
19. Strassburger, J. and Breuer, M. M., *J. Soc. Cosmet. Chem.*, 1985, **36**, 61.
20. Naito, S., *Sen-i Gakkaishi*, 1985, **41**(4), 120.
21. Erra, P., Gomez, N., Dolcet, L. M., Julia, M. R., Lewis, D. M. and Willoughby, J. H., *Textile Res. J.*, 1997, **67**(6), 397.
22. Nishikawa, N., Tanizawa, Y., Tanaka, S., Horiguchi, Y., Matsuno, H. and Asakura, T., *Polymer Commun.*, 1997, **39**(4), 1001.
23. Fraser, R. D. B. and MacRae, T. P., *Conformation in Fibrous Proteins and Related Synthetic Polypeptides*. Academic Press, 1973, pp. 469–525.
24. Suzuki, E., Crewther, W. G., Fraser, R. D. B., MacRae, T. P. and McKern, N. M., *J. Mol. Biol.*, 1973, **73**, 275.
25. Amiya, T., Miyamoto, T. and Inagaki, H., *Biopolymers*, 1980, **19**, 1093.
26. Sakabe, H., Miyamoto, T. and Inagaki, H., *Sen-i Gakkaishi*, 1981, **37**(7), 273.
27. Asakura, T., Kuzuhara, A., Tabata, R. and Saito, H., *Macromolecules*, 1985, **18**(10), 1841.
28. Ishida, M., Asakura, T., Yokoi, M. and Saito, H., *Macromolecules*, 1990, **23**(1), 88.
29. Yoshimizu, H. and Asakura, T., *J. Appl. Polym. Sci.*, 1990, **40**, 1745.
30. Asakura, T., Demura, M., Uyama, A., Ogawa, K., Komatsu, K., Nicholson, L.K. and Cross, T.A., *Silk polymers: material science and biotechnology*. ACS Symposium Series, 1994, **544**, 148–154.
31. Asakura, T., Demura, M. and Nishikawa, N., eds G.A. Webb and I. Ando, *Annual Reports on NMR Spectroscopy*, 1997, **34**, 302–346.
32. Kricheldorf, H. R. and Muller, D., *Colloid Polym. Sci.*, 1984, **262**, 856.
33. Yoshimizu, H. and Ando, I., *Macromolecules*, 1990, **23**, 2908.
34. Yoshimizu, H., Mimura, H. and Ando, I., *Macromolecules*, 1991, **24**, 862.
35. Yoshimizu, H., Mimura, H. and Ando, I., *J. Mol. Struct.*, 1991, **246**, 367.
36. Mack, J. W., Torchia, D. A. and Steinert, P. M., *Biochemistry*, 1988, **27**, 5418.
37. O'Donnel, I. J. and Thompson, E. O. P., *Aust. J. Biol. Sci.*, 1964, **17**, 973.
38. Dowling, L. M. and Crewther, W. G., *Prep. Biochem.*, 1974, **4**(3), 203.
39. Hilterhaus-Bong, S. and Zaha, H., *Int. J. Cosmet. Sci.*, 1987, **9**, 101.
40. Tanaka, S., Iimura, H. and Sugiyama, T., *J. Soc. Cosmet. Chem. Jpn.*, 1992, **25**(4), 232.
41. Pauling, L., Corey, R. B. and Branson, H. R., *Proc. Natl. Acad. Sci. U.S.*, 1951, **37**, 205.
42. Rao, D. R., *J. Appl. Polym. Sci.*, 1992, **46**, 1109.
43. Nishikawa, N., Tanizawa, Y., Tanaka, S., Horiguchi, Y., Matsuno, H. and Asakura, T., *Polym. J.*, 1998, **30**(2), 125.
44. Miyazawa, T. and Blot, E. R., *J. Am. Chem. Soc.*, 1961, **83**, 712.
45. Koenig, J. L. and Frushour, B., *Biopolymers*, 1972, **11**, 1871.
46. Chen, M. C. and Lord, R. C., *J. Am. Chem. Soc.*, 1974, **96**, 4750.